UNCLASSIFIED

[redacted]

[redacted]

170

2261-6023-T8-000

APOLLO BLOCK I

TASK MSC/TRW ASPO-19

# AS-201
# SPACECRAFT 009
# PROPULSION PERFORMANCE EVALUATION
# (U)

NAS 9-4810

22 APRIL 1966

CLASSIFICATION CHANGED TO Unclassified
By Authority of TRW Letter BM-4 dtd 2/10/67
By C. Jakobut Date 9/26/67



TRW SYSTEMS

[redacted]

UNCLASSIFIED

TRW - 2261-6023-T8-000
22 April 1966
TOTAL PAGES: 49

# AS-201
# SPACECRAFT 009
# PROPULSION PERFORMANCE EVALUATION
# (U)

Prepared Under Contract
NAS 9-4810



Prepared by

Performance Analysis Section

APPROVED: D W Vernon

D. W. Vernon, Head
Propulsion Performance Analysis Section



TRW Systems
One Space Park
Redondo Beach, California

# FORWARD

This program technical report is submitted to NASA/MSC in accordance with Task MSC/TRW A-19, Contract NAS 9-4810. It contains the final propulsion performance evaluation and malfunction analyses of the Service Propulsion System of AS 201 and supersedes both the AS 201 propulsion performance quick look report which was published on 15 March 1966, and the revised quick look report which was published on 23 March 1966. The cooperation of the Propulsion Analysis Section of NASA/MSC and, in particular, the efforts of Mr. Pat B. Burchfield in coordinating activities between NASA/MSC and TRW Systems and providing needed information has been greatly appreciated.

TABLE OF CONTENTS



TOTAL PAGES: 49

LIST OF FIGURES

# AS-201
# SPACECRAFT 009
# PROPULSION PERFORMANCE EVALUATION

## I. INTRODUCTION

This report is submitted in fulfillment of Task A-19, Subtask III-11, Item K, Final Post-Flight Performance and Malfunction Analysis Report, of Contract NAS9-4810. Item K calls for "preparation and submittal of documentation which presents the results of final post-flight performance and malfunction analyses within forty days after receipt of all necessary flight data." The minimum data required to perform a final propulsion performance analysis of the SPS from flight of the first Apollo-Saturn 201 mission were received from NASA/MSC on 12 March 1966, requiring final propulsion performance evaluation input by 23 April 1966.

A significant effort by TRW Systems in the areas of malfunction analysis and propulsion system performance evaluation has been expended, the results of which are discussed herein. A matrix describing potential malfunction hypotheses versus the substantiating telemetry data is given, and a discussion of two phase flow which would result from helium ingestion into the oxidizer feed system is presented. Also included is a general discussion of the BEPP (Best Estimate of Propulsion Parameters) Program, flight test data used in the analysis, SPS performance simulation, and the propulsion/propellant systems performance parameters as derived from the BEPP analysis. In addition, a discussion of the data processing required to produce thrust acceleration from both sources of axial acceleration is included, i.e., the data processing of measurements CH3184 Delta Velocity Remaining Potentiometer Output and CK0004 Linear Acceleration Structure X-Axis is included.

## II. SUMMARY

Mission AS 201 was flown from the Merritt Island Launch Area on 26 February 1966. Flight data were reduced from three telemetry receiving stations: KSC, Ascension and RKV. Data from the RKV were used for ignition and the first 160 seconds of the SPS first burn only, due to poor data quality after 160 seconds. Data from Ascension was used for the remainder of the first burn and the second burn.

A malfunction was observed to start at first burn ignition plus 70 seconds and continue throughout both burns causing the actual velocity gained from the SM/SPS to be less than required. All probable malfunctions were investigated, and helium ingestion was found to be the only malfunction that could have caused all of the abnormal transients observed in the telemetered data. Helium was first ingested at 70 seconds. Increasing amounts of helium ingested during the remainder of the flight caused the observed transients in the telemetered data and resulted in the failure of the SM/SPS to achieve the required velocity gain. It was concluded that the most probable source of the helium leak was in the oxidizer transfer line standpipe inside and near the top of the zero-g can.

The Best Estimate of Propulsion Performance (BEPP) Program was used to determine the propulsion system performance parameters during the steady state portion of the SPS first burn. The resulting propulsion system performance parameters are presented herein. Two sources of axial acceleration were used in an attempt to calculate accurate total thrust acceleration profiles for use in the BEPP Program, but the inaccuracy of the resulting profiles were an order of magnitude higher than data on past missile programs. The lack of accurate thrust acceleration data degraded the resulting performance reconstructions from the BEPP Program. Thus, the derived AS 201 SPS propulsion system performance parameters are not considered to necessarily represent the true performance of the propulsion system.

The classical methods of calculating rocket engine performance have also been exercised. These methods are discussed and the results presented.

## III. ANOMALY ANALYSIS

The following matrix brings together all the SPS performance malfunction hypotheses that have been considered and shows which data confirm or deny each hypothesis. The individual hypotheses are described briefly in the lefthand column of the matrix, while the top row identifies the principal propulsion performance data functions. Where a given function can be explained by a particular malfunction hypothesis, an X is placed in the appropriate cell. Otherwise, it is left blank. Each malfunction hypothesis is discussed in subsequent sections of the report. Helium ingestion, which has the strongest data confirmation, is analyzed in detail in a separate section.

### A. Helium Ingestion Through Leak in Oxidizer Standpipe

Helium ingestion in the oxidizer feed system inside the zero-g can would explain all of the transient characteristics indicated by the data. A time increasing volumetric ratio of helium to oxidizer would cause the velocities to increase in the feed system, the mass flowrate of oxidizer to be decreased and the pressure drop from the tank to the oxidizer valve inlet to increase. The decreased oxidizer valve inlet pressure and oxidizer mass flowrate would cause the chamber pressure to decrease, which would cause the fuel mass flowrate to increase and the fuel valve inlet pressure to decrease. The propellant level dropping in the oxidizer tank would provide an increasing driving force which would cause the increasing helium flowrate necessary for this mechanism. A quantitative investigation of helium ingestion effects was undertaken and is presented in the Helium Ingestion Section, Section III.

The gradual decay of 5° F. in oxidizer valve inlet temperature and feed line temperature could be explained by cold helium bubbles in the oxidizer providing a large heat transfer area allowing the fluid-gas mixture temperature

TABLE III-1

CORRELATION OF HYPOTHESIZED ANOMALIES WITH TELEMETERED ABNORMAL DATA TRANSIENTS

| Malfunction Hypothesis | Telemetered Abnormal Data Transients | | | | | | | | | |
|---|---|---|---|---|---|---|---|---|---|---|
| | Chamber Pressure (First Burn) | Fuel Tank Pressure | Oxidizer Tank Pressure | Fuel Interface Pressure | Oxidizer Interface Pressure | Chamber Pressure (Second Burn) | Helium Storage Tank Pressure | Oxidizer Tank Pressure Decay At Cutoff | Oxidizer Engine Feed Line Temperature (First Burn) | Oxidizer Engine Feed Line Temperature (Second Burn) |
| A. Helium Ingestion through leak in oxidizer stand-pipe | X | X | X | X | X | X | X | X | X | X |
| B. Helium ingestion through leak in top of zero-G can | X | X | X | X | X | X | X | X | X | X |
| C. Partial constriction in helium supply | | X | X | X | X | | X | X | | |
| D. Partial constriction in transfer line between oxidizer storage and sump tanks | | X | X | X | X | | X | X | | |
| E. Complete constriction in transfer line between oxidizer storage and sump tanks | | X | X | X | | | | | | |
| F. Complete constriction in helium supply line down-stream of tank pressure transducer | | X | X | X | | | | | | |
| G. Thrust chamber throat errosion | X | X | X | X | X | | X | | | |
| H. Oxidizer leak upstream of propellant shutoff valves | X | X | X | X | X | | X | | | |
| I. Oxidizer leak downstream of propellant shutoff valves | X | X | X | X | X | | X | | | |

to decrease. The temperature would decrease with increasing proportions of helium.

The erratic chamber pressure during the second burn could be the result of a large amount of helium being ingested into the oxidizer during the zero-g period between the two burns of the SPS Engine. After the first few seconds of the second burn, a large volumetric proportion of helium could have passed through the oxidizer feed line. This large volumetric proportion of helium could also account for the $10^{\circ}$ F. short duration drop in the oxidizer feed line temperature. The low chamber pressure would cause a corresponding decrease in valve inlet pressures, which was observed. The short duration decrease of $10^{\circ}$F. observed in the feed line temperature was not indicated in the oxidizer inlet temperature. This is due to the fact that the oxidizer inlet temperature was measured on the external surface of the feed line. Thus, the transducer would not detect the short duration temperature change. The indicated constant oxidizer tank pressure until 185 seconds, followed by a sharp drop of 16 psi and the similar drop after the second burn, is considered to be the result of more helium being ingested with the oxidizer than the helium supply system could provide, i.e., the flow from the helium storage tanks is limited by the maximum flowrate through the pressure regulators.

One mechanism for helium to flow into the zero-g can would be a break in the standpipe near the top of the zero-g can. Excessive vibrations were noted in Service Module Systems integration tests at the White Sands Test Facility. If these vibrations were close to the natural frequency of the standpipe or the propellant utilization system probe, similar vibrations on Spacecraft 009 could have resulted in a leak in the transfer line inside the zero-g can. The leak could be through a break in a standpipe at the top of the zero-g can. If the break occurred just inside the top of the zero-g can, the pressure drop of the

oxidizer flowing through the can would allow helium to flow into the zero-g can with a head of liquid above the can. The estimated pressure drop through the can to the suspected point of helium ingestion near the top is approximately 0.7 psi, and the pressure due to the oxidizer head above the can at 70 seconds is approximately 0.8 psi. The head of liquid above the can is approximately equal to the pressure drop through the can at 70 seconds; therefore, helium ingestion could have started at that time.

During the FRF, a leak was observed that allowed oxidizer to flow from the sump tank to the storage tank. The leak was reported to be due to a faulty seal between the oxidizer transfer line between the sump and storage tanks and the standpipe in the sump tank; however, the actual location of the leak was not confirmed. The seal is located near the bottom of the zero-g can and could allow helium to flow into the zero-g can. However, the pressure drop through the zero-g can to the seal is approximately 0.4 psi and the pressure due to the oxidizer head above the location of the seal at 70 seconds is approximately 3.0 psi. Therefore, the location of the leak was most likely near the top of the zero-g can.

Although the means for flowing helium into the zero-g can is uncertain, helium ingestion is the only mechanism that explains all of the transients observed in the telemetered data and the reported value of oxidizer loaded in the tank. Thus, it is concluded that helium ingestion near the top of the zero-g can is the most probable cause of the anomaly.

B. Helium Ingestion Through Leak in Top of Zero-g Can

The same arguments presented in Section A are valid for the mechanism of a leak in the top of the zero-g can, except helium would not enter the zero-g can until the oxidizer level dropped below the level of the top of the can. The implication of the top of the zero-g can uncovering at SPS first burn igni-

tion plus 70 seconds is that approximately 8,900 pounds of oxidizer was loaded instead of the reported 10,460 pounds. The pressure drop from the ullage through the top of the zero-g can would be positive after the can is uncovered, resulting in an increasing flowrate of helium into the can as the liquid level drops in the sump tank. However, subsequent analysis using the BEPP program has indicated that the reported oxidizer loaded weight is approximately correct. Thus, it is concluded that this malfunction is not the cause of the anomaly.

C. Partial Constriction in Helium Supply Line, Downstream of Tank Pressure Transducer

A partial constriction in the helium supply line (possibly in the heat exchanger) would explain part of the transient characteristics indicated by the data. To reproduce the observed oxidizer valve inlet pressure, the pressure drop due to the constriction would have to increase with burn time, e.g., an accumulation of foreign material, beginning initially at SPS first burn plus 70 seconds. The indicated valve inlet pressure drop minus the approximate head loss is 14 psi between 70 and 185 seconds, and the reported nominal helium supply line pressure drop is 6 psi. Thus, for this mechanism, the oxidizer tank pressure would decrease 20 psi after shutdown, which is 4 psi lower than the drop indicated by the data. In addition, the chamber pressure between 70 and 185 seconds does not appear to be driven by the valve inlet pressures, i.e., the chamber pressure indicated by the valve inlet pressures would be much higher than the observed values, which is not explained by this mechanism. In addition, the start transient characteristics and the quasi-steady state level of the chamber pressure during the second burn cannot be explained by this mechanism.

Although some of the anomalies can be explained by a partial constriction in the helium supply line downstream of the oxidizer tank pressure transducer, the observed chamber pressure and the magnitude of the oxidizer tank pressure drop during both shutdowns cannot be explained by this mechanism. The observed erratic chamber pressure during the second burn requires an additional malfunction. Therefore, it is considered extremely unlikely that this malfunction occurred.

D. Partial Constriction in Transfer Line, Between Oxidizer Storage and Sump Tanks

A partial constriction between the oxidizer storage and sump tanks would explain part of the transients indicated by the telemetered data. For this mechanism, a decay in oxidizer valve inlet pressure would result until the pressure was reached which would allow the storage tank pressure to maintain the sump tank at a lower steady state value. If the constriction increased with time, the observed oxidizer valve inlet pressure could be reproduced. At shutdown the storage tank ullage pressure would expand into the sump tank, and the indicated tank pressure would be reduced by approximately one-half of the difference between the sump and storage tank pressures. The additional pressure drop due to the constriction would have to be 14 psi, which is the observed valve inlet pressure drop minus the approximate head loss. This would contribute a 7 psi drop to the indicated tank pressure loss at shutdown. The reported nominal helium supply line pressure drop is 6 psi; therefore, the total expected tank pressure drop would be 13 psi, which compares favorably to the observed drop in oxidizer tank pressure of 16 psi. However, the chamber pressure during the first burn does not appear to be driven by the inlet pressures, i.e., the chamber pressure would only drop to 90 psia in response to the decays in valve inlet pressures. In addition, the start transient

characteristics and the quasi-steady state level of the chamber pressure during the second burn cannot be explained by this mechanism. It is also highly improbable that a constraint would develop in a two and one-half inch diameter line. Therefore, it is considered extremely unlikely that this malfunction occurred.

E. Complete Constriction in Transfer Line Between Oxidizer Storage and Sump Tanks

If there werea complete constriction between the oxidizer storage and sump tanks that developed at SPS first burn ignition plus 70 seconds, the oxidizer valve inlet pressure would decay to approximately 92 psia at first burn shutdown. The helium storage tank pressure would be constant after ignition plus 70 seconds, and the oxidizer tank pressure would remain constant through shutdown. However, the indicated oxidizer interface pressure, after correcting for a reported bias, only dropped to 137 psia; the helium storage tank pressure dropped continuously through the entire burn, and the oxidizer tank pressure dropped 16 psi at shutdown. Therefore, it is considered that this malfunction did not occur.

F. Complete Constriction in Helium Supply Line, Downstream of Tank Pressure Transducer

If there were a complete constriction between the oxidizer storage and sump tanks that developed at SPS first burn ignition plus 70 seconds, the oxidizer valve inlet pressure would decay to approximately 120 psia at first burn shutdown. The helium storage tank pressure would be constant after ignition plus 70 seconds, and the oxidizer tank pressure would be constant through shutdown. However, the oxidizer interface pressure only dropped to 137 psia; the helium storage tank pressure dropped continuously through the entire burn; and the oxidizer tank pressure dropped 16 psi at shutdown. Therefore, it is considered that this malfunction did not occur.

G. Thrust Chamber Throat Erosion

An erosion of the thrust chamber throat would cause the chamber pressure to decrease, the propellant flowrates to increase and both inlet pressures to decrease by approximately the same magnitude. However, the thrust would also increase, and for a throat area increase of the magnitude indicated by the chamber pressure drop, the propellants would probably be depleted before the end of the scheduled burn time. For this mechanism, the required velocity would be reached earlier than expected; however, the indicated velocity gain was over 20 percent less than the expected velocity increase. In addition, the chamber pressure during the second burn returned to over 90 psia, indicating that the throat had not enlarged. The indicated decrease in the oxidizer tank pressure at shutdown would require an additional malfunction. Although some of the observed trends would be expected from a thrust chamber throat erosion, it is considered that this malfunction did not occur.

H. Oxidizer Leak Upstream of Propellant Shutoff Valves

An oxidizer leak upstream of the shutoff valves would cause an increased oxidizer flowrate, a corresponding decrease in oxidizer valve inlet pressure, and somewhat smaller decreases in chamber pressure and in fuel valve inlet pressure. Part of the decrease in chamber pressure would be in response to the decrease in the inlet pressure. A somewhat compensating effect would result from a decrease of the oxidizer line and injector pressure drop due to the reduced engine flowrate. The size of the leak that would result in the observed transients during the first burn could be uniquely determined, but all of the observed anomalies would not result from an oxidizer leak, so the computation was not undertaken. The oxidizer tank and valve inlet pressures were constant between burns, and if an oxidizer leak were present, these pressures would

have decayed. The chamber pressure of over 90 psia could not have been obtained during the second burn if a leak were present, and the oxidizer tank pressure drop of 16 psia at shutdown would require an additional malfunction. Although certain of the observed transients during the first burn could be explained by an oxidizer leak upstream of the propellant shutoff valves, other unexplained anomalies indicate that this malfunction did not occur.

I. Oxidizer Leak Downstream of Propellant Shutoff Valves

An oxidizer leak downstream of the propellant shutoff valves could cause certain of the indicated transients during the first burn. The oxidizer tank and valve inlet pressures would be constant between burns, since the propellant shutoff valves would prevent oxidizer from leaking between burns. However, the chamber pressure during the second burn would not increase to 90 psia, and the oxidizer tank pressure decay of 16 psia at shutdown would remain unexplained. However, the hole size would have to increase with time during the latter portion of the first burn in order to cause the indicated oxidizer interface and chamber pressure profiles during that time period. At the start of the second burn, the same hole size that was present during the end of the first burn would be expected. Thus, the same interface and chamber pressures would be expected at the start of the second burn except for the effects of any tank pressure equalization between the sump and storage tanks during the zero-g period due to the flow resistance between them. The pressures would then be expected to decay from this level during the second burn.

The oxidizer interface pressure and the chamber pressure are greater at the start of the second burn, and the drop to 10 psia chamber pressure during the second burn recovered to a level greater than the level observed

during the end of the first burn, indicating that a leak was not present. Although certain of the observed transients during the first burn could be explained by an oxidizer leak downstream of the propellant shutoff valves, other unexplained anomalies tend to indicate that the malfunction did not occur.

## IV. HELIUM INGESTION ANALYSIS

Flight data indicates the pressure in the oxidizer tank remains approximately constant through the total first burn, while the oxidizer inlet pressure drops significantly beginning at SPS ignition plus 70 seconds. The pressure in the fuel tank remains approximately constant, and the fuel inlet pressure drops slightly. Computer calculations utilizing an SPS influence coefficient engine model with inputs of flight data inlet pressures predict a chamber pressure profile (Figure 1) which drops much less severely than the flight data indicates. The lowest first burn chamber pressure data is 70 psia at 183 seconds, while the value predicted by engine influence coefficient model is 90 psia for the inlet pressures indicated at that time. Therefore, C-star, the total weight flow, or both are less than predicted by the mathematical engine model.

R. C. Martinellis' paper entitled, "Isothermal Pressure Drop for Two-Phase Two Component Flow in a Horizontal Pipe," (Reference 1) indicates the pressure drop, in two-phase flow of gas and liquid for given fluid flowrates, can be much greater than for the flow of gas or liquid alone. This lends credence to the possibility of helium ingestion explaining the observed data. Sufficient helium ingestion in the oxidizer feed system could result in reduced oxidizer liquid flowrate into the engine, reducing the chamber pressure, and resulting in a larger than nominal pressure drop from the tank to interface, even at the reduced liquid flowrate. Hand calculations of the oxidizer flowrate were made using the indicated thrust chamber ($P_{ci}$) and fuel inlet ($P_{if}$) pressures, assuming the fuel inlet to thrust chamber resistance ($R_{fic}$) remains constant. Solving the following simultaneous equations for C-star (C*) graphically for the conditions indicated at the time of 183 seconds (see Figure 2):

$$C^* = \frac{P_{cn} A_t g}{\dot{w}_o + \dot{w}_f} \quad (1)$$

$$C^* = 4825.0 + 922.5 \frac{\dot{w}_o}{\dot{w}_f} - 325.0 \left(\frac{\dot{w}_o}{\dot{w}_f}\right)^2 \quad (2)$$

(relationship derived from multiple linear regression analysis of SPS static test data)

where,

$$\dot{w}_f = \sqrt{\frac{(P_{if} - P_{ci})\,\rho_f}{R_{fic}}} = \text{fuel flowrate, lbm/sec} \quad (3)$$

$\dot{w}_o$ = oxidizer flowrate, lbm/sec

$A_t$ = thrust chamber throat area from the predicted time history, $in^2$

$P_{cn}$ = throat stagnation pressure derived from telemetered data

$P_{ci}$ = injector end stagnation pressure

Utilization of Equation (2) (C-star based entirely on the liquid mixture ratio) must be qualified somewhat. The helium ingestion even at large helium volumetric flowrates would not degrade the value of C-star significantly due to thermochemical considerations. However, Equation (2) was derived from a range of mixture ratios from 1.48 to 2.28 and may not be accurate at the low mixture ratios (approximately 1.0) calculated for the last portion of the SPS first burn. In addition, the effects of helium is the oxidizer on the fluid distribution and the injector impingement angles in the injector would reduce the C-star efficiency. Thus, the oxidizer flowrates calculated using this equation are probably somewhat smaller than actual values. This calculation indicates that the oxidizer flowrate could be decreased greatly, and the fuel flowrate would rise only slightly, thus the low total flowrate and the reduced C-star efficiency would result in a low chamber pressure.

Solving the equations at T = 183 seconds where,

$P_{io}$ = 136 psia, $P_{if}$ = 145, $P_{ci}$ = 70.0, $A_t$ = 119.96

from Equation (3):

$\dot{w}_f$ = 25.07 lb/sec

and from simultaneous solution of Equations (1) and (2) (Figure 2),

$\dot{w}_o$ = 21.8 lb/sec

Using Martinelli's method of analysis (References 1 and 2) the magnitude of the volumetric flowrate of helium necessary to give the observed tank to interface pressure drop at T = 183 seconds, with above calculated oxidizer liquid flowrate was determined.

Equation (3) of Reference 2 gives:

$$\left(\frac{\Delta P}{\Delta L}\right)_{TPF} = \left(\frac{\Delta P}{\Delta L}\right)_{L} \Phi_{Ltt}^{2}$$

where,

$\left(\frac{\Delta P}{\Delta L}\right)_{TPF}$ = pressure gradient for two-phase flow

$\left(\frac{\Delta P}{\Delta L}\right)_{L}$ = pressure gradient assuming only liquid phase flowing (for the given liquid flowrate)

$\Phi_{Ltt}$ = the experimental parameter plotted in Figure 2 of Reference 2 versus the independent modulus $X_{tt}$, which is an independent parameter which correlates well with experimental two-phase pressure drops, and is given by:

$$X_{tt} = \left(\frac{\mu_L}{\mu_g}\right)^{0.111} \left(\frac{V_L}{V_g}\right)^{0.555} \left(\frac{W_L}{W_g}\right)$$ = the dimensionless two-phase flow independent parameter in which the flow of both the liquid and the gas is turbulent.

For this equation,

$\mu_L, \mu_g$ = viscosity of liquid and gas respectively

$V_L$, $V_g$ = specific volume of the liquid and gas respectively

$W_L$, $W_g$ = weight flow of the liquid and gas respectively

The calculations at T = 183 seconds were performed as follows:

From the flight data, the pressure drop from the oxidizer tank to engine inlet in the period before 70 seconds is 18.2 psia. The engine model calculates an oxidizer flowrate of 44.0 pounds per second in this steady state region. At T = 183 seconds, where $\dot{w}_o$ = 21.8 pounds per second, $(\Delta P)_L$ would therefore be

$$(\Delta P)_L = \frac{(21.8)^2}{(44)^2} \quad (18.2) = 4.55 \text{ psia}$$

The observed $\Delta P$ is 158 - 138.5 = 19.5. Therefore, using the equation

$$(\Delta P)_{TPF} = (\Delta P)_L \ \Phi_{Ltt}^{\ 2}$$

$$19.5 = 4.55 \ \Phi_{Ltt}^{\ 2}$$

therefore,

$$\Phi_{Ltt}^{\ 2} = 4.30$$

$$\Phi_{Ltt} = 2.08$$

From Reference 2, Figure 2, this gives:

$$\sqrt{X_{tt}} = 2.35$$

therefore,

$$X_{tt} = 5.5 = \left(\frac{\mu_L}{\mu_g}\right)^{0.111} \left(\frac{V_L}{V_g}\right)^{0.555} \left(\frac{W_L}{W_g}\right)$$

$$5.5 = \left(\frac{0.423}{0.018}\right)^{0.111} \left(\frac{0.158}{90.2}\right)^{0.555} \left(\frac{W_L}{W_g}\right)$$

$$5.5 = \frac{1.42}{40.2} \left(\frac{W_L}{W_g}\right)$$

therefore,

$$\frac{W_L}{W_g} = \frac{(40.2)(5.5)}{1.42} = 156$$

$$W_g = \frac{21.8 \text{ lb/sec}}{156} = 0.056 \text{ lb/sec}$$

at the given pressure, assuming thermal equilibrium with the propellant, the helium volumetric flowrate would be:

$$V = 1.20 \text{ ft}^3/\text{sec}$$

At 21.8 lb/sec, the oxidizer volumetric flowrate is 0.242 $ft^3$/sec; therefore, the percent by volume of helium flowing is 83 percent.

This helium flowrate, calculated for the conditions indicated at T = 183 seconds, is the maximum helium ingestion rate determined for the first burn. During the second burn, when the $P_c$ is indicated to have dropped to 10 psia, the volumetric percent for that period is estimated to be 90 to 95 percent (no calculation was made).

Subsequent to the initial calculations indicated above, computer calculations were made utilizing the LEMDE non-linear engine model. In these calculations the oxidizer flowrate history between 70 and 183 seconds was calculated on the basis of the telemetered interface pressures, and the chamber pressure. The program used a constant fuel interface-to-chamber resistance and varied the oxidizer interface-to-chamber resistance to lower the oxidizer flowrate during the period of helium ingestion. The assumption

was made in these calculations that the C-star as a function of mixture ratio relationship derived from static testing at AEDC was valid. The telemetered data indicates the oxidizer tank pressure at first burn shutdown is 160 psia. Assuming the tank pressure drops linearly from 174 to 160 psia during the first burn, and using the inlet pressures and the flowrates calculated using the above procedure, the helium ingestion rate was determined using Reference 2, Figure 2. The results are plotted in Figure 3.

The oxidizer main valve inlet temperature and the feed line temperature drops 5° F. from T = 70 seconds to the end of the first burn. This could be due to the increasing percentage of cool helium flowing through the system. A 10° F. drop in the feed line temperature occurs during the middle portion of the second burn. This occurs at the same time as the chamber pressure drop to 10 psia, both of which could be explained by a slug containing a large percentage of helium going through the feed system into the engine at this time.

Integration of the helium flowrate in Figure 3 yields a total helium loss of 72.9 $ft^3$ or 8.5 pounds. An independent calculation was made of the total helium loss from the vehicle during the first burn, using the thermodynamic states of the helium storage tanks and propellant tanks at startup and shutdown. The volume of helium remaining in the propellant tanks at shutdown for this calculation was determined from the BEPP Program predicted oxidizer and fuel mass remaining at first burn shutdown. This calculation yields 6.1 pounds total helium loss, assuming final helium temperature in the tank of 12° F. If a helium temperature of 62°, equal to the propellant temperature, is assumed, the mass loss determined by this method would be 12.9 pounds. The actual temperature is probably between these two values, and therefore the results by both methods are in good agreement, definitely indicating helium was lost from the pressurization and propellant tankage systems.

An approximate calculation was made of the pressure drop in the oxidizer retention reservoir from the reservoir entrance to the reservoir top. This calculation assumed loss of the complete velocity head at the reservoir entrance turn and the turn at the top of the reservoir, yielding a loss of 0.4 psia and 0.3 psia respectively, for a total of 0.7 psia. A leak between the transfer line and the inside of the reservoir would result in helium flow into the reservoir when the pressure in the reservoir at the leak point becomes less than in the line. Helium ingestion begins occurring at T = 70 seconds, and the net fluid head due to propellant above the top of the reservoir at this time point is calculated to be 0.8 psia at the thrust acceleration indicated by data. These two calculations and the calculated time increasing helium ingestion rate indicate that a leak from the transfer line to the reservoir near the top of the reservoir can explain the observed data.

# V. PROPULSION SYSTEM PERFORMANCE EVALUATION

## A. Discussion of BEPP Program

The TRW developed Best Estimate of Propulsion Parameters (BEPP) Program was used to determine the AS-201 SPS performance parameters. This program utilizes a weighted, least-squares technique in conjunction with all of the available data from static test in addition to the physical laws which describe the behavior of the propulsion/propellant systems and their interaction with the spacecraft. From the various flight and static-test-derived data, the simulation calculates the time histories of thrust acceleration, propellant weight consumed, inert weight expended, and the propulsion system performance parameters. The simulation embodies complete error models for the various flight and static test data used as inputs. The technique is to determine the values of the propulsion and propellant systems performance parameters in the error model that minimize the quantity:

$$X^2 = \sum_{j=1}^{n} \frac{(Z_j^* - Z_j)^2}{\sigma_j^{*2}}$$

where,

$X^2$ = an arbitrary function to be minimized

$Z_j^*$ = a flight test data point

$Z_j$ = value corresponding to the flight test data point calculated by the simulation

$\sigma_j^*$ = a priori estimate of the standard deviation of the data point

## B. Types of Flight Data Used

The flight test data are divided into the following three classes:

(1) statistically matched constraints

(2) imposed flight data from the particular flight

(3) standard spacecraft class parameters

Class (1) data are those matched statistically in a weighted least-squares sense. These data consist of the following:

Thrust acceleration time history

CM/SM damp weight

Loaded oxidizer weight

Loaded fuel weight

Class (2) data are those derived from each flight test which are used as input to the propulsion and vehicle simulation of BEPP and consist of the following:

SPS Engine start and cutoff times

Propellant density time histories

Propellant interface pressure time histories

Oxidizer line resistance time history

SPS nozzle throat area time history

Class (3) data are the standard spacecraft class parameters used as input to the propulsion and vehicle simulations of BEPP which consisted of the following:

SPS Engine influence coefficients

Miscellaneous flowrate schedule (ablative nozzle flowrate, RCS flowrates, etc.)

C. SPS Performance Simulation

The standard influence coefficient model for the SPS performance simulation was utilized from ignition to 70 seconds. Thereafter, this model

could not be used due to the anomalous behavior of the oxidizer interface pressure and the thrust chamber pressure which did not follow the influence coefficient model. Therefore, an auxiliary engine balance-rebalance program (LEMDE model) was used to simulate the anomalous oxidizer flow phenomena by determining the variable oxidizer inlet to chamber resistance required to match the telemetered oxidizer and fuel interface pressures and chamber pressure. The resulting oxidizer line resistance time-history after ignition +70 seconds was then input into the BEPP model to simulate the changes in thrust and propellant flowrates which were not adequately modeled by the standard use of influence coefficients.

D. Determination of Total Thrust Acceleration Profile

Total thrust acceleration profiles were calculated from two axial accelerometers: (1) CK 0004, linear acceleration structure x-axis, and (2) CH 3184, $\Delta V$ remaining potentiometer output. The engine gimbal angles: (1) CH 0034, pitch position feedback input, and (2) CH 1034, yaw position feedback input, were used to calculate the total thrust acceleration along the engine axis. Each acceleration data source had specific advantages that were used to produce the best estimate of total thrust acceleration. The processing is discussed in the following two sections.

(1) CH 3184, $\Delta V$ Remaining Potentiometer Output:

The total thrust acceleration was calculated using the equation:

$$a_t = -(dV_g / dt)(\cos \Theta)^{-1} (\cos \phi)^{-1} \qquad (1)$$

where,

$a_t$ = total resultant thrust acceleration, ft/sec

$V_g$ = velocity to be gained measured along the x-axis, ft/sec

$t$ = time from Range Zero, sec

$\theta$ = angle between the SPS Engine and the x-axis in the pitch plane, degrees

$\phi$ = angle between the SPS Engine and the x-axis in the yaw plane, degrees

Measurement CH 3184 data came from the axial accelerometer in the body mounted attitude gyro assembly. The accelerometer was assumed to be aligned to the x-axis within the specified 14 arc minutes. An on-board system integrates the acceleration and differences the resulting velocity from a specified terminal velocity, giving the velocity to be gained ($V_g$), which was telemetered as a proportional voltage. This data was scaled to units of feet per second in the format received by TRW. The time derivative of $V_g$ was calculated using a polynomial differentiating filter. This procedure gave values of $dV_g/dt$ throughout the SPS burn for use in Equation (1). The pitch and yaw angles through which the SPS Engine deviated from the x-axis were read directly from measurements CH 0034 and CH 1034, respectively. The cosines of these angles were used in Equation (1).

The data editing procedure was designed to eliminate obviously erroneous points and to cope with the least-count problem imposed by the telemetry. A change in the telemetered velocity was only indicated when a change of at least 55 feet per second had been accumulated since the previous level. Data were selected only at the times when a velocity change was registered. Since a given velocity change could have been accumulated at any time in the 100 milliseconds sampling period, the time was biased -50 milliseconds.

Several different polynomial differentiating filters were evaluated. One-hundred one data points in a second degree polynomial moving arc fit was considered the best for smoothing the data from this flight.

(2) CK 0004, Linear Acceleration Structure X-Axis:

This acceleration data source showed two distinct advantages over measurement CH 3184 data. Firstly, the output was telemetered as acceleration, which eliminates the noise-producing differentiation step required in the CH 3184 data processing. Secondly, the 100 samples per second sampling rate for this measurement as compared to a 10 samples per second rate for measure CH 3184 tends to eliminate the telemetry-induced resolution problem, encountered on measurement CH 3184 data.

The data were edited, smoothed with a numerical filter, scaled by 32.174, and corrected for the engine gimbal angles. As was anticipated, a significant zero shift was observed. The magnitude of this zero shift changed during SPS burn from 5.99 feet per second squared to 5.70 feet per second squared. The zero drift was assumed to be linear, and the data were corrected accordingly. Since the CH 3184 data were not as susceptible to zero drift, the CK 0004 data profile was bias corrected such that the velocity gain during a convenient time period was the same for both sources. This correction was 158 feet per second out of a total 2,989 feet per second during the period between 1,226 and 1,365 seconds.

Basically then, the thrust accelerations used in the final BEPP Program calculation have the shape of CK 0004 data (scale corrected for zero drift during the firing) and the magnitude of CH 3184 data.

E. Analysis Results

Acceleration data derived primarily from measurement CK 0004 and calibrated against measurement CH 3184 as a standard were matched in the BEPP Program from 1,213 seconds to 1,300 seconds. Figure 6 presents the flight acceleration data match (BEPP Program derived minus actual, divided by actual, in percent) versus time at one second intervals throughout the SPS burn duration. Compared to a typical Titan II, Stage 2 analysis (see Figure 4), the noise in the acceleration is quite excessive. Most of the Titan deviations from zero are within $\pm$ 0.25 percent. The band of $\pm$ 0.25 percent is plotted in Figure 6 for a ready comparison between expected acceleration matches when good acceleration data are available and the acceleration match obtained on AS-201.

The importance of good acceleration data is illustrated by a comparison of BEPP Program results when the two different acceleration data sources are utilized. All BEPP Program inputs were identical for both calculations with the exception of the total thrust acceleration profiles. A comparison of Figure 5 which presents the CH 3184 acceleration data match to Figure 6 which presents the CK 0004 acceleration data match shows the increased magnitude of noise present in the measurement CH 3184 data. Since the BEPP Program matches the acceleration data in a least squares sense in deriving the key propulsion parameters of thrust, specific impulse, mixture ratio, and propellant flowrates, the noise and inaccuracy in acceleration data is reflected into the propulsion parameters. This accounts for the differences observed in Table V-1.

Table V-1

| Propulsion Parameters (1) | Acceleration Source | | Δ |
|---|---|---|---|
| | CK 0004 (2) | CH 3184 (3) | |
| F (lbs) | 21,277 | 20,934 | 343 |
| Isp (sec) | 308.2 | 304.7 | 3.5 |
| $\mu$ (o/f) | 2.006 | 2.000 | 0.006 |
| $\dot{w}_f$ (lb/sec) | 46.08 | 45.81 | 0.27 |
| $\dot{w}_o$ (lb/sec) | 22.97 | 22.90 | 0.07 |

(1) At standard inlet conditions.

(2) Time span in the acceleration data match 1213 - 1300.

(3) Time span in the acceleration data match 1226 - 1300. The later initial time was necessitated by the long smoothing span required for this data.

Although the mixture ratios from both calculations are nearly equal, their validity is questionable since only initial propellant loaded weights are known, and there is no other measurement of propellant quantities during the flight. Thus, there is no data to drive the BEPP solution from the input reported values of initial propellant weights. The difference in specific impulse values is significant and is due primarily to the poor quality of the acceleration data and the lack of sufficient instrumentation for accurate flowrate determinations.

The BEPP Program results from measurement CK 0004 are considered to be the more realistic. This acceleration data actually combines the best features of both data sources.

The final BEPP Program results which are considered to be most representative of the propulsion system performance of AS 201 are summarized in Table V-2. Plots which describe the time histories of the acceleration match and the derived propulsion parameters are given in Figures 6 through 11.

The acceleration data from measurement CK 0004 is matched by the BEPP Program during the flight time span of 1,213 to 1,300 seconds. The resulting delta acceleration match is presented in Figure 6. The delta acceleration profile during the region being matched is primarily bounded by plus or minus two percent. The larger delta accelerations after the region being matched is plotted for a comparison of input to BEPP Program derived acceleration, but they do not affect the BEPP Program derived propulsion system performance parameters. The deviations are the result of the engine model's not being able to accurately describe the helium ingestion, e.g., the effects of helium ingestion on C-star and $C_f$ have not been included in the model. If the additive effect of the helium in the thrust chamber gasses were properly considered, the calculated thrust would be greater during the latter portion of the first burn. This would raise the calculated acceleration gain rate during the latter portion of the first burn and improve the flight acceleration data match after 1,320 seconds.

Table V-II

04/21/66

BEPP RUN NO. 201/SPS BEPP PROGRAM RESULTS ENGINE SN AJ-10-137

| QUANTITY | SPECIFICATION VALUE | MEASURED VALUE | MEASURED VALUE σ | MEASURED VALUE REFERENCE | BEPP VALUE | BEPP σ | DEVIATION (p-r) | PER CENT DEVIATION (p-r)/r | $I_{sp}$, sec |
|---|---|---|---|---|---|---|---|---|---|
| ENGINE PERFORMANCE | | | | | | | | | |
| $F_v$, lb | 21500.00 | 21430.00 | 71.000 | | 21277.42 | 42.4 | -152.58 | -.712 | |
| $F_{vac}$, lb | | .00 | | | | | | | |
| $I_{sp_v}$, sec | 311.05 | 310.60 | | | 308.16 | 3.0 | -2.44 | -.786 | |
| $I_{sp_i}$ | | 310.40 | | | 308.16 | | -2.24 | -.722 | |
| $I_{sp_i}$ | | | | | 308.62 | | | | |
| $I_{sp_i}$ | | | | | | | | | |
| $I_{sp_i}$ | | | | | | | | | |
| $MR_v$, unitless | 2.0000 | 2.0100 | .007 | | 2.0063 | | -.0037 | -.184 | |
| $MR_i$ | | | | | 1.4143 | | | | |
| $\Delta MR_{fb}$ | | | | | -.5957 | | | | |
| $\Delta MR_{ox}$ | | | | | -.5920 | | | | |
| $\dot{w}_{ox}$, lb/sec | 46.08 | 46.05 | | | 46.08 | 1.00 | .03 | .064 | |
| $\dot{w}_{fu}$, lb/sec | 23.04 | 22.96 | | | 22.97 | 0.99 | .01 | .032 | |
| $\dot{w}_{cp}$, lb/sec | 69.12 | 69.01 | | | 69.05 | | .04 | .053 | |
| $TR_1$ | | | | | 99.80 | | | | |
| Outage, lb | | | | | .00 | | | | |
| Outage, per cent | | | | | .000 | | | | |
| $\Delta t_{imp}$, sec | | | | | -1395.60 | | | | |
| $I_{sp}$, lb-sec | | 5318.00 | | | -.00 | | -5318.00 | -100.000 | |
| MIXTURE, LEVEL SHIFTS, VERNIER GAIN AND CONSTRAINED $\Delta I_{sp}$'s | | | | | | | | | $I_{sp}$, sec |
| $W_p$, lb | | 18828.00 | 20.000 | | 18828.01 | | .01 | .000 | .0000 |
| $W_{ox}$, lb | | 10245.00 | 35.000 | | 10245.43 | 34.97 | .43 | .004 | |
| $W_{fu}$, lb | | 4662.00 | 18.000 | | 4662.11 | 18.00 | .11 | .002 | |
| $W_{ti}$, lb | | 33735.00 | 44.000 | | 33735.55 | 39.63 | .55 | .002 | |
| $V_{ox1}$, ft$^3$ | .50 | .00 | .000 | | .00 | | -.00 | -.000 | -.0000 |
| $V_{fu1}$, ft$^3$ | | .00 | | | .00 | | -.00 | -.000 | -.0000 |
| $V_{ox2}$, ft$^3$ | .50 | .00 | .000 | | .00 | | -.00 | -.000 | .0000 |
| $V_{fu2}$, ft$^3$ | | .00 | | | .00 | | -.00 | -.000 | .0000 |
| $V_{ox3}$, ft$^3$ | | | | | | | | | |
| $V_{fu3}$, ft$^3$ | | | | | | | | | |
| $V_{ox4}$, ft$^3$ | | | | | | | | | |
| $V_{fu4}$, ft$^3$ | | | | | | | | | |
| $\Delta v$, ft/sec | | 1864.59 | | | 1864.66 | | .07 | .004 | |
| SUM TOTAL OF $\Delta I_{sp}$'s | | | | | | | | | |
| CORRECT TOTAL $\Delta I_{sp}$ | | | | | | | | | |
| MEASURE OF TOTAL INPUT DATA NOISE: CHI SQUARED | | | | | 0.61142 | | | | |

UNCLASSIFIED

F. Additional SPS Performance Calculations

In addition to the BEPP Program method of determining SPS performance, the classical methods for calculating rocket engine performance have been exercised. These methods include determining engine specific impulse using the following equations:

$$I_{sp} = \frac{\Delta V}{g_o \ln\left(\frac{M_i}{M_f}\right)} \tag{1}$$

$$I_{sp} = \frac{C^* C_f}{g_o} \tag{2}$$

$$I_{sp} = \frac{F}{\dot{w}_t} = \frac{C_f P_c A_t}{\left(\frac{\rho_o \Delta P_o}{R_o}\right)^{1/2} + \left(\frac{\rho_f \Delta P_f}{R_f}\right)^{1/2}} \tag{3}$$

where,

$\Delta V$ = total velocity gain during the time interval of interest, ft/sec

$g_o$ = weight to mass conversion factor, 32.174, $ft/sec^2$

$M_i$ = total mass of the stage at the start of the time interval of interest, lbm

$M_f$ = total mass of the stage at the end of the time interval of interest, lbm

$C^*$ = thrust chamber characteristic exhaust velocity, ft/sec

$C_f$ = thrust chamber thrust coefficient, unitless

$\dot{w}_t$ = total propellant flowrate, lb/sec

$P_c$ = thrust chamber nozzle stagnation pressure, psia

$A_t$ = thrust chamber throat area, $in^2$

$\rho_o$, $\rho_f$ = oxidizer and fuel propellant density respectively, $lb/ft^3$

$\Delta P_o$, $\Delta P_f$ = oxidizer and fuel interface-to-chamber pressure drop respectively, psi

$R_o$, $R_f$ = oxidizer and fuel interface-to-chamber flow resistance, respectively, $sec^2/in^2\text{-}ft^3$

1. Method Using Equation (1)

Results obtained from Equation (1) were calculated from the velocity gained as indicated by the integrated axial accelerometer data (measurement CH 3184) from SPS ignition (T) to T + 77.52 seconds. The mass ratio, $M_i/M_f$, was calculated from (1) the BEPP Program results and (2) the integrated flowrates derived from the pressure drops from the interfaces to the combustion chamber, assuming nominal stage damp weights, propellant tanked weights and interface-to-chamber resistances. The controlling factor which degrades the accuracy of this method is the least count of $\Delta V$ from the integrated axial accelerometer output due to the PCM telemetry capability. The total output range in terms of velocity to be gained is -1000 to + 13000 fps. The minimum increment that can be resolved is $(1/2)^8$ of the full 14,000 fps scale or about 55 fps. This lack of precision translated into terms of equivalent $I_{sp}$ during the time duration considered amounts to 10.3 seconds equivalent $I_{sp}$ precision. In other words, an error of only one PCM count in the time interval chosen for this calculation produces an error of 10.3 seconds of $I_{sp}$. Therefore, this method does not permit an accurate determination of engine performance.

2. Method Using Equation (2)

Both C-star and $C_f$ are strong functions of engine mixture ratio and weak functions of chamber pressures. Therefore, the engine flowrates were calculated at 20 second increments using the measured $\Delta P$'s from interface to chamber, assuming constant line resistances during the first 70 seconds of burning. The resulting MR values were used to calculate $C_f$ from the

theoretical relationship as follows:

$$C_f = 1.753 + 0.0961\ MR - 0.01965\ MR^2$$

The values of C-star at each mixture ratio were obtained from Reference 3 for the L-Series of static test firings at AEDC. The pressure dependence of both C-star and $C_f$ was not considered since the chamber pressure was approximately nominal during this time interval.

3. Method Using Equation (3)

The engine thrust was calculated from the head end measured $P_c$ after correcting for the predicted loss from head end pressure to nozzle stagnation pressure. Theoretical values of $C_f$ determined using the method described for Equation (2) were also used for this case. The engine flowrates were calculated using the measured $\Delta P$'s as also described above. Propellant densities were determined from the telemetered temperatures measured at the tank exits. Line resistances were assumed constant during the 70 second time interval and were based upon the acceptance test values as calculated from the engine log book.

4. Summary of Calculated Performance Results

The specific impulse values given in Table V-2 are shown for reference purposes only and do not constitute the TRW Systems recommended values of flight derived engine performance.

Table V-2

| Method | SPS Engine Performance Parameters | | | |
|---|---|---|---|---|
| | Average (T to T+77.52) | | Standard Inlet Cond. | |
| | Thrust (lb) | $I_{sp}$ (sec) | Thrust (lb) | $I_{sp}$ (sec) |
| 1. Equation (1) | | | | |
| a. $\ln (M_i/M_f)$ from BEPP | 20655 | 317.0 | 22010 | 320.6 |
| b. $\ln (M_i/M_f)$ from $\int \dot{w} dt$ using $\Delta P$ | 20630 | 316.1 | 21975 | 319.7 |
| 2. Equation (2) | 20470 | 313.7 | 21805 | 317.3 |
| 3. Equation (3) | 21120 | 323.7 | 22490 | 327.3 |

# VI. FIGURES

Figure 1
MEASURED AND PREDICTED PRESSURE PROFILES

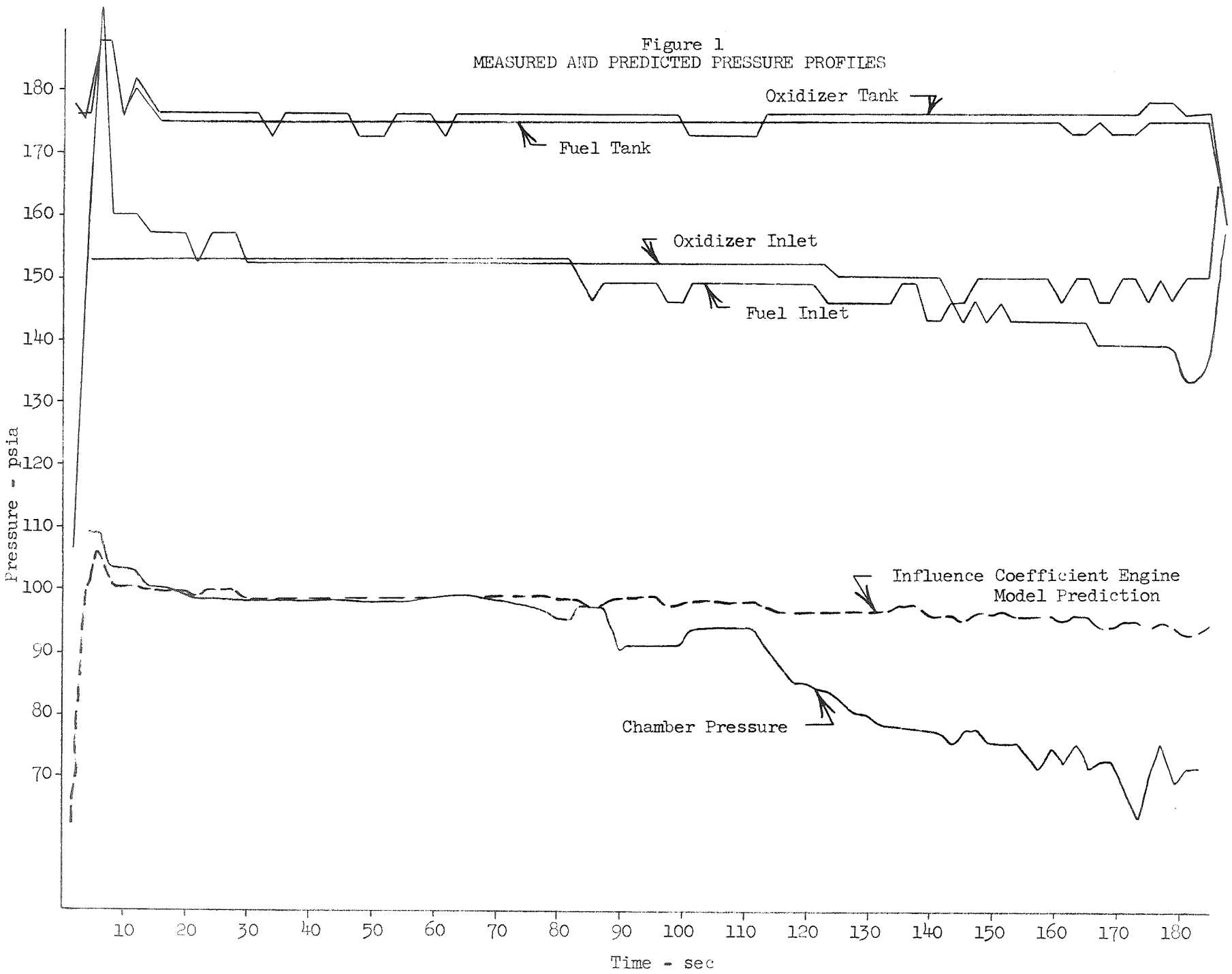

Figure 2

GRAPHICAL SOLUTION
FOR
OXIDIZER FLOWRATE AT 183 SECONDS
($\dot{w}_f$ = 25.07)

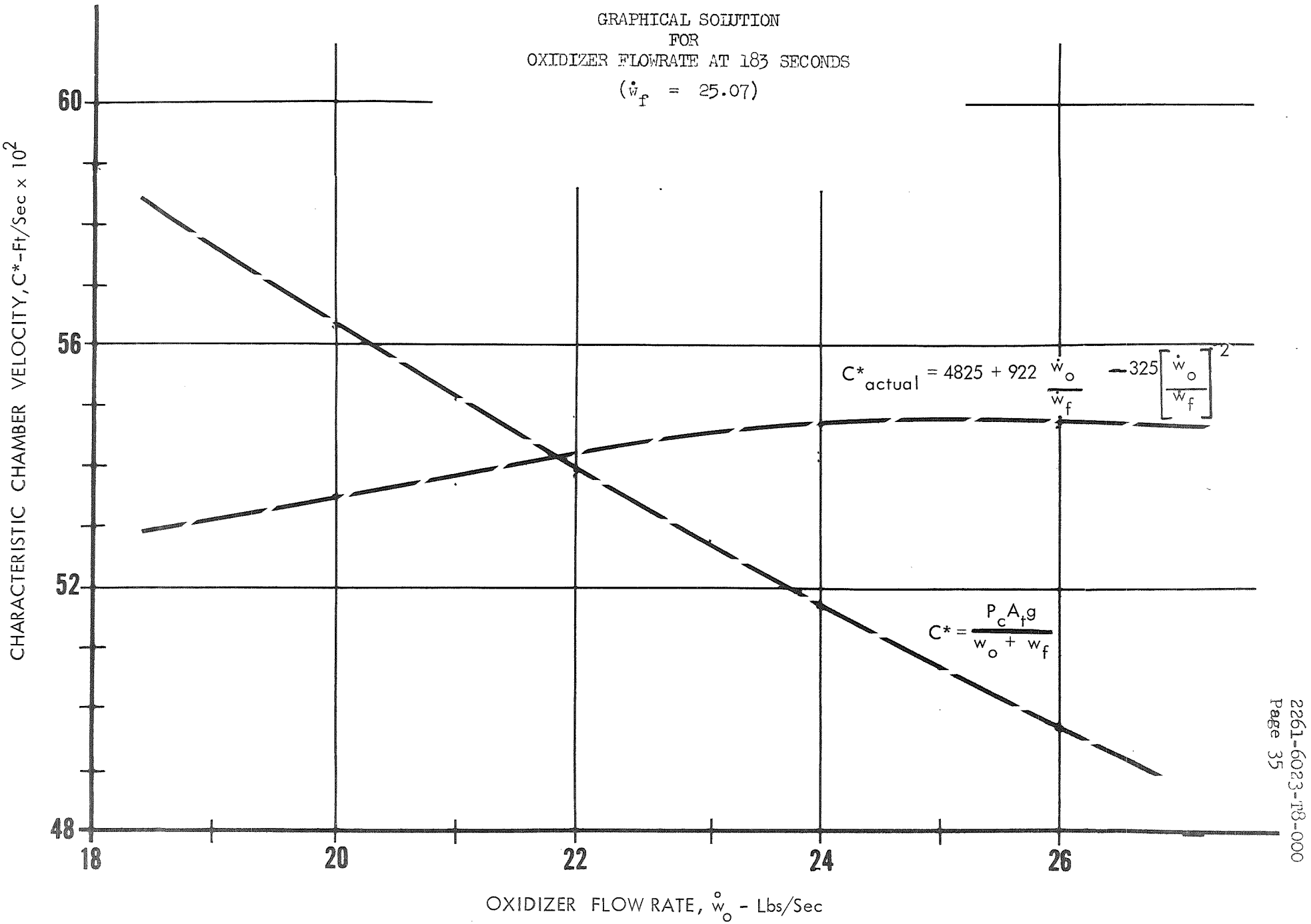

Figure 3

HELIUM INGESTION RATE
VERSUS TIME

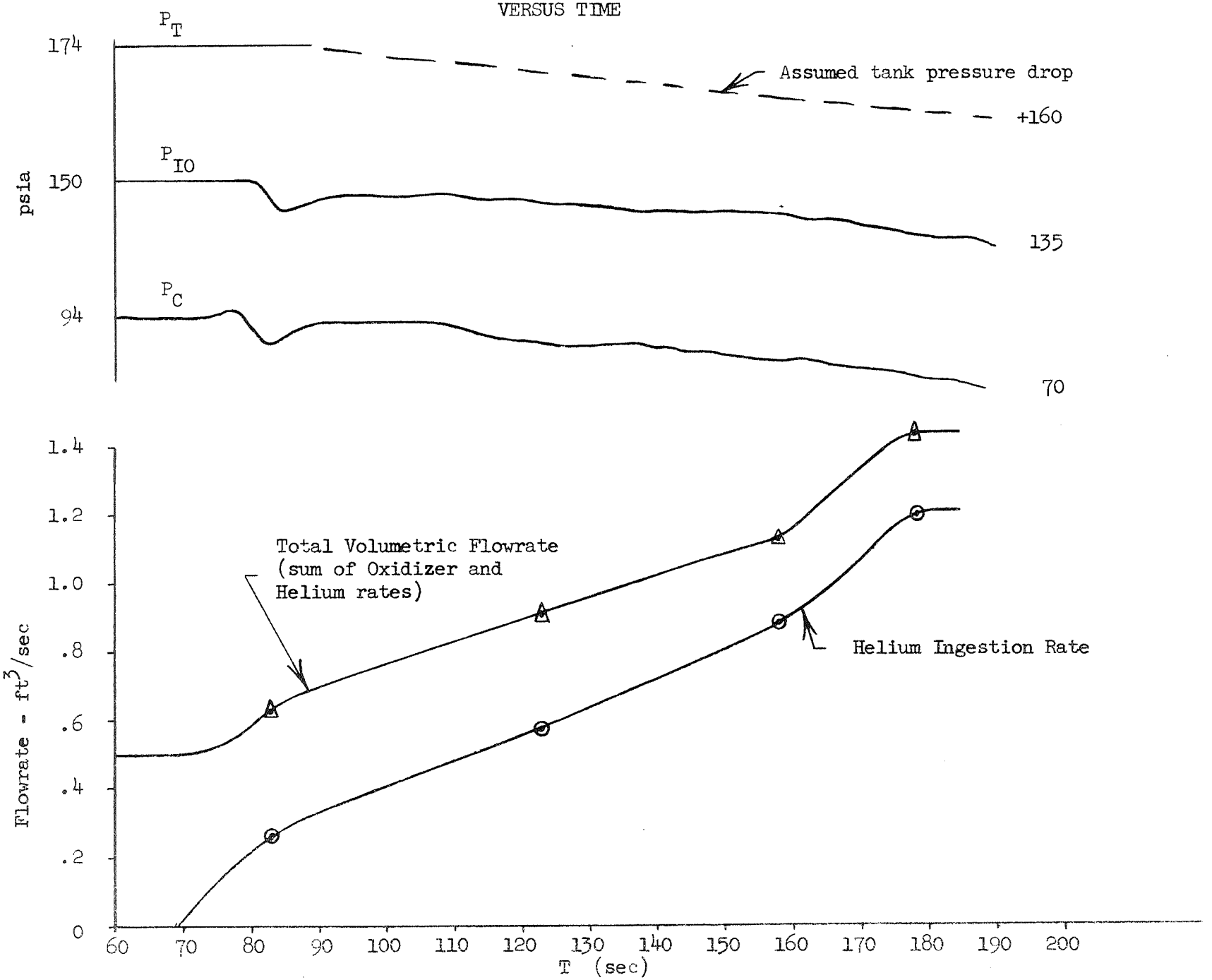

[redacted]

TRW

B-62 STAGE II PROPULSION PARAMETERS

DELTA ACCELERATION MATCH

FIGURE 4

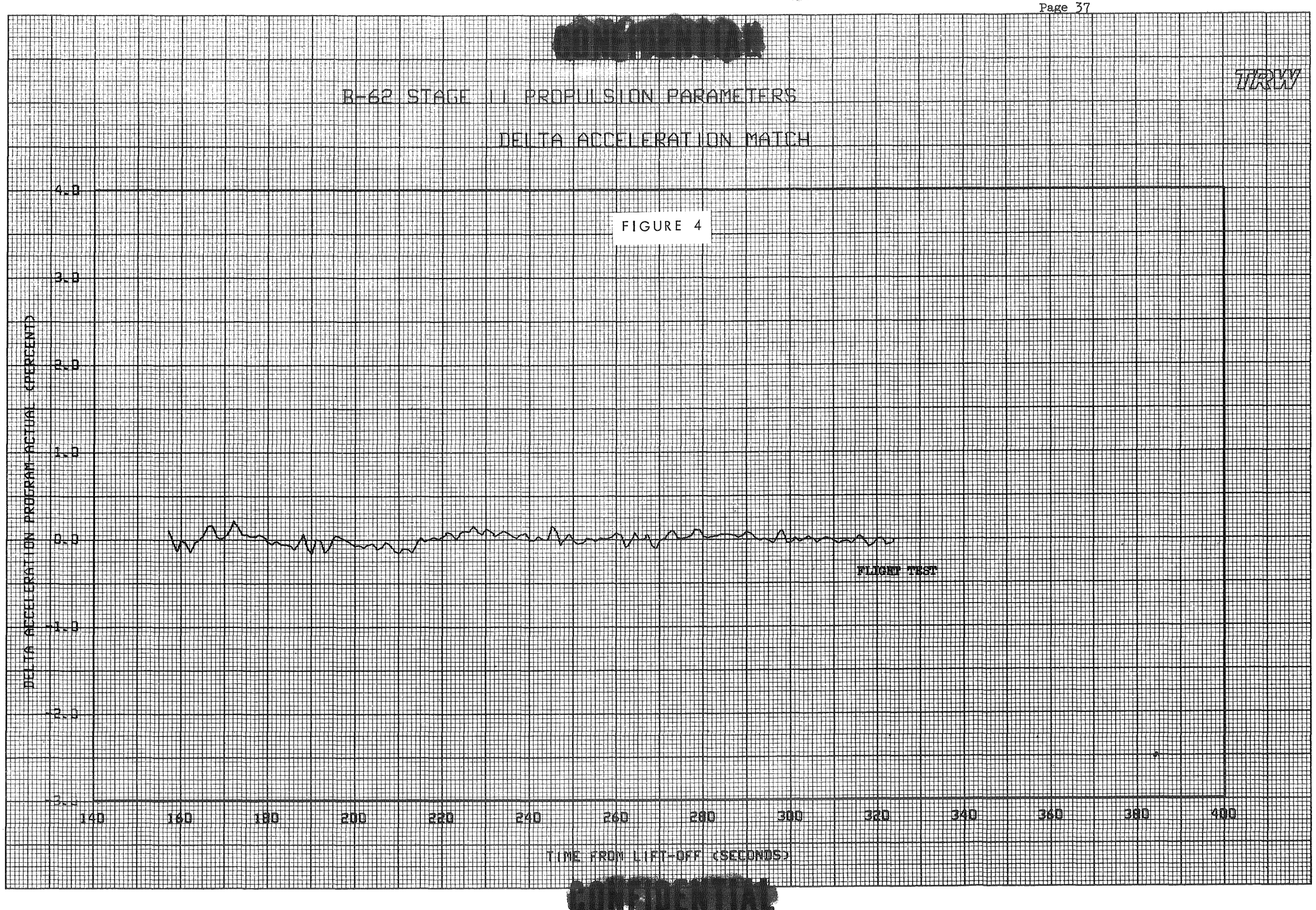

[redacted]

TRW

MISSION AS 201 SPS PROPULSION PERFORMANCE PARAMETERS

DELTA ACCELERATION MATCH

DELTA V REMAINING

FIGURE 5

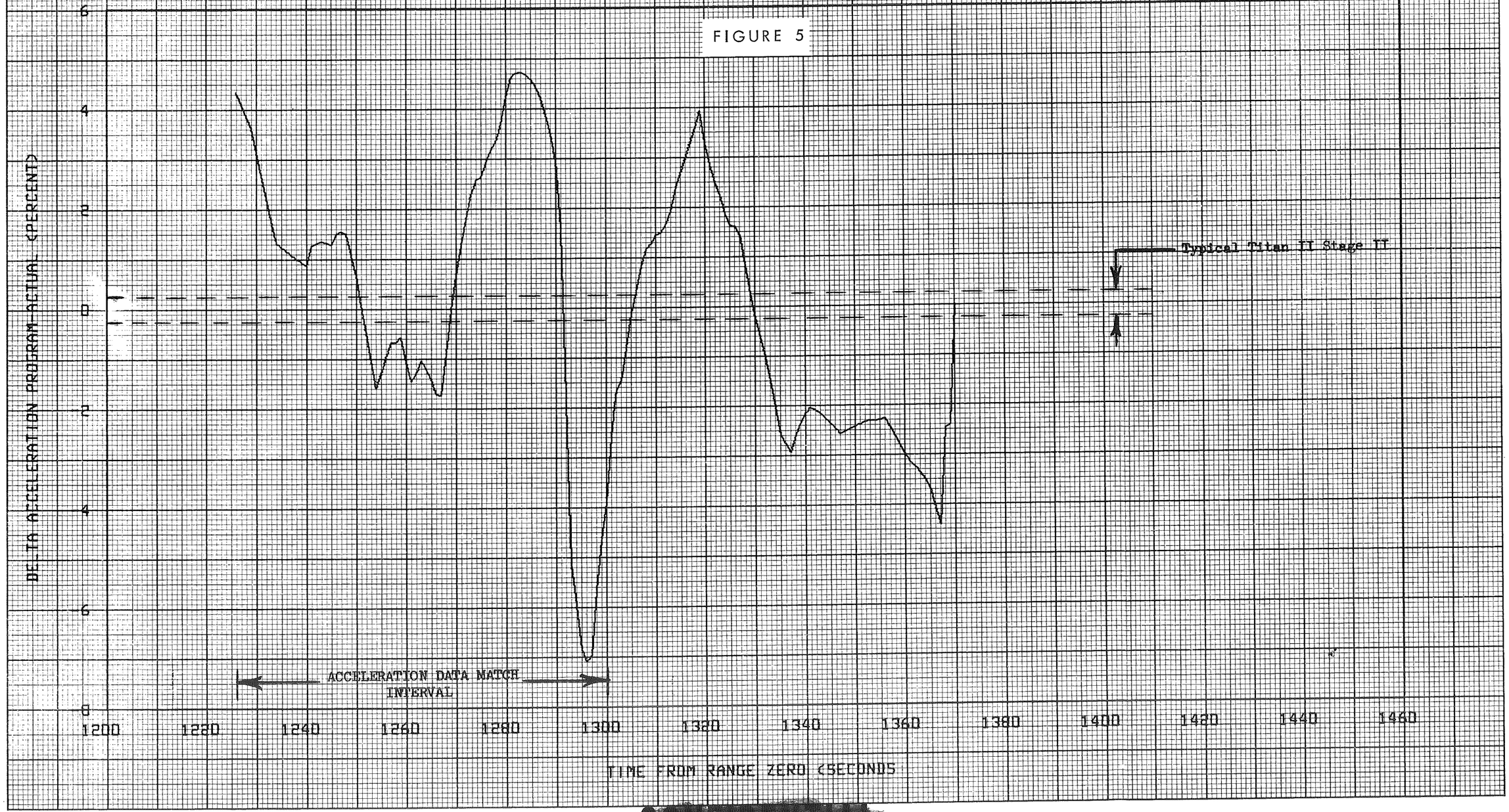


[redacted]

[redacted]

MISSION AS 201 SPS PROPULSION PERFORMANCE PARAMETERS

DELTA ACCELERATION MATCH

CK0004 CORR

TRW

FIGURE 6

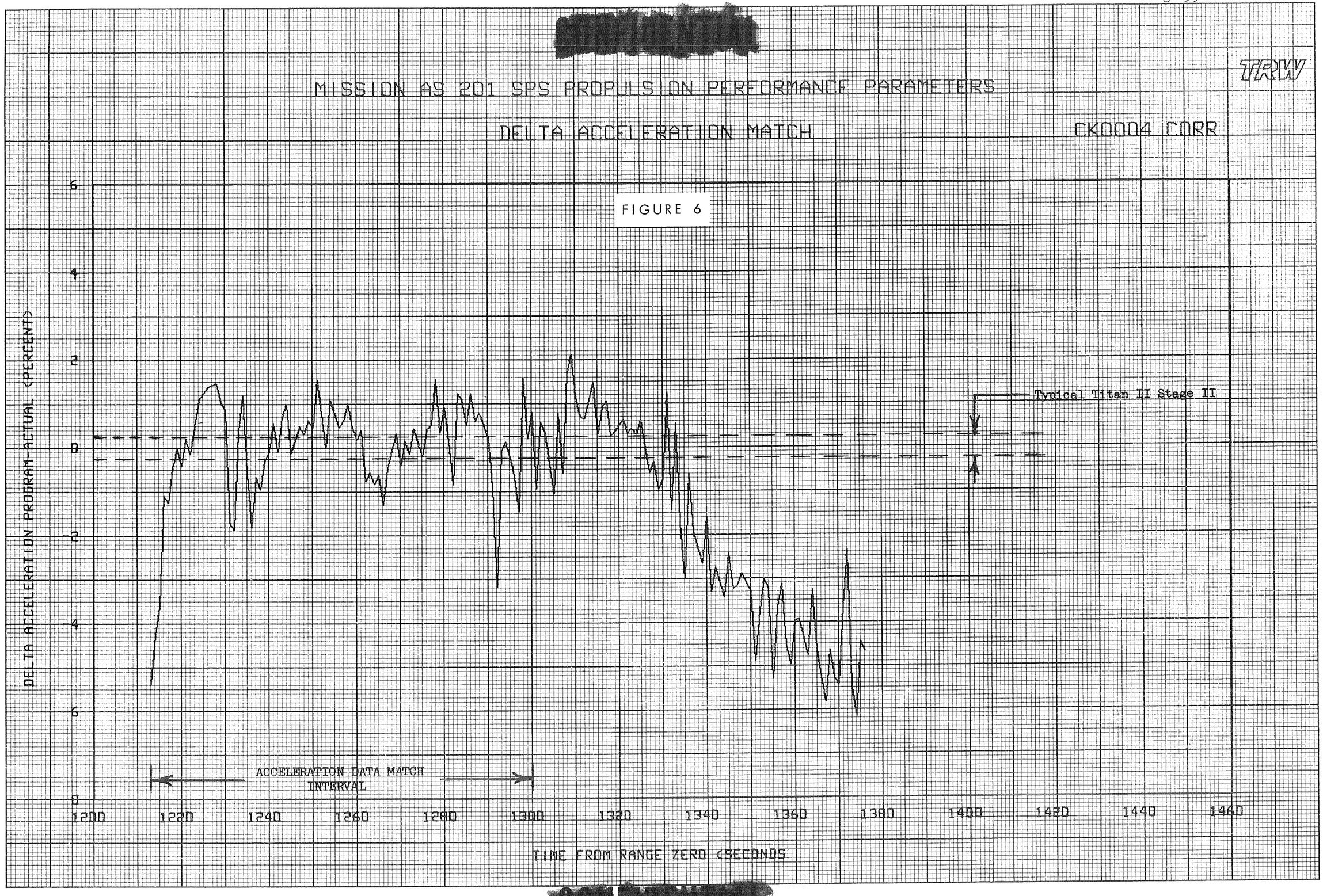


[redacted]

[redacted]

MISSION AS 201 SPS PROPULSION PERFORMANCE PARAMETERS

TRW

VEHICLE THRUST CK0004 CORR

FIGURE 7

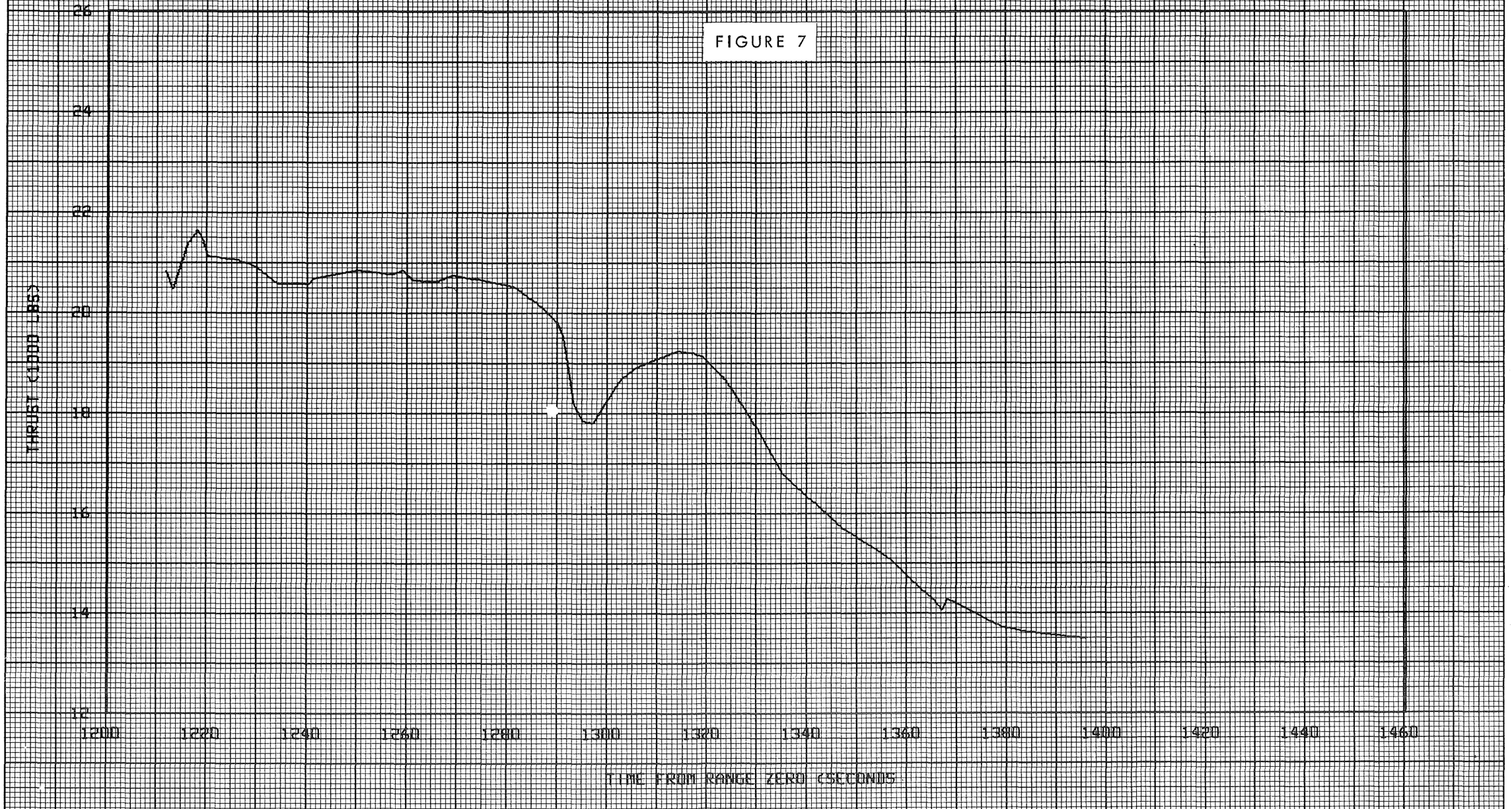


[redacted]

[redacted]

TRW

MISSION AS 201 SPS PROPULSION PERFORMANCE PARAMETERS

VEHICLE SPECIFIC IMPULSE CK00004 CORR

FIGURE 8

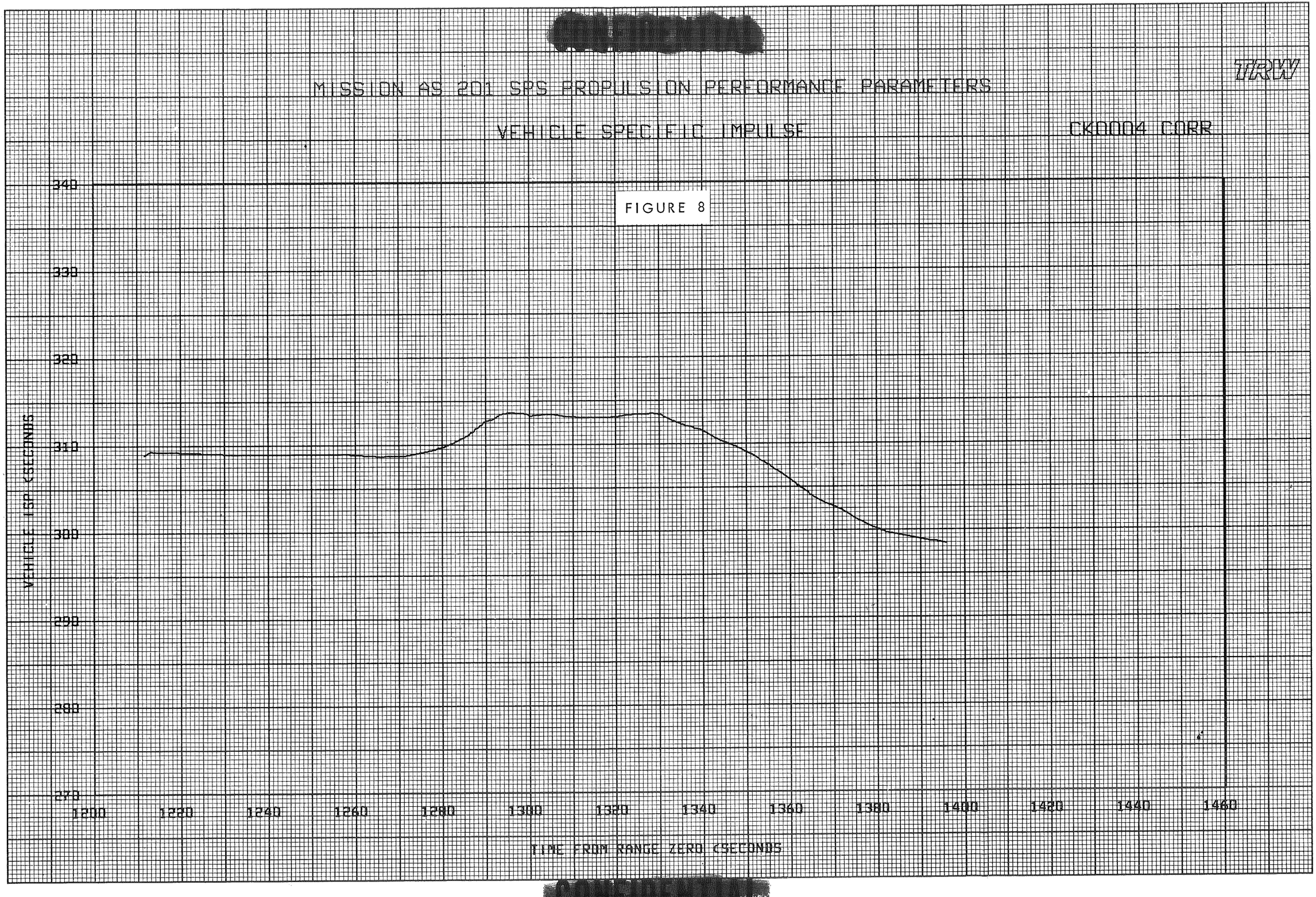


[redacted]

[redacted]

TRW

MISSION AS 201 SPS PROPULSION PERFORMANCE PARAMETERS

MIXTURE RATIO CK0004 CORR

FIGURE 9

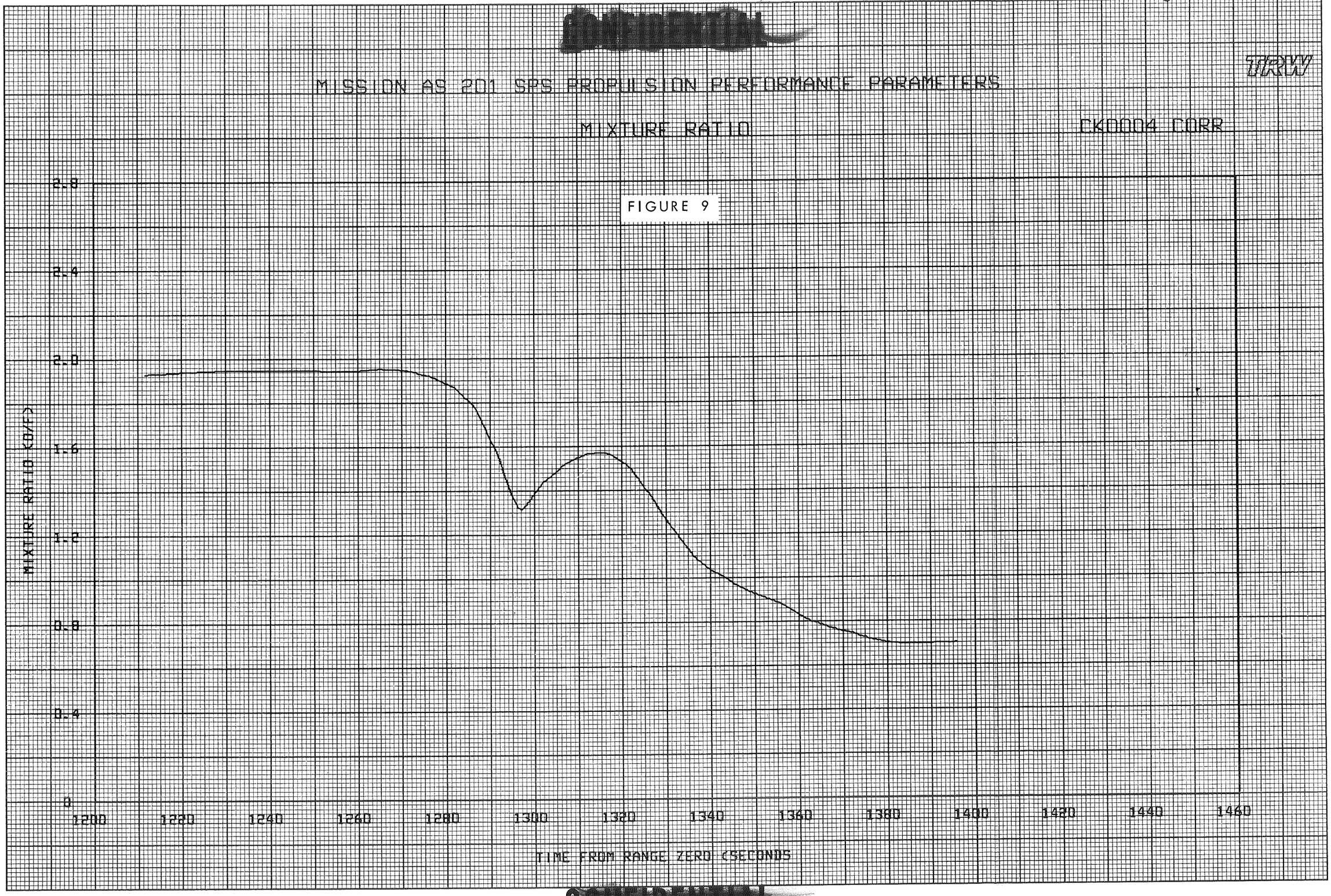

[redacted]

MISSION AS 201 SPS PROPULSION PERFORMANCE PARAMETERS

TRW

OXIDIZER FLOW RATE CK0004 CORR

FIGURE 10

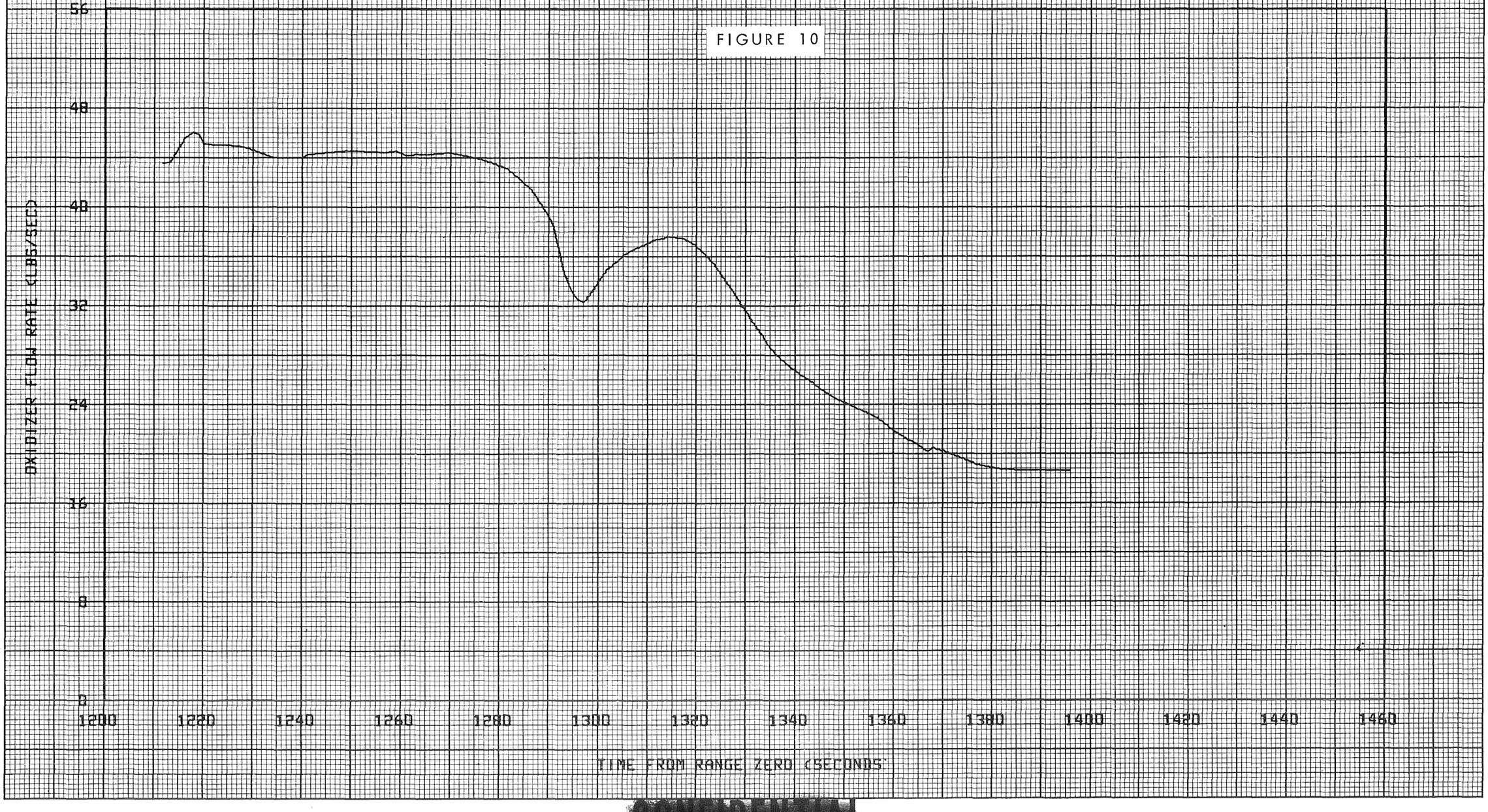

[redacted]

MISSION AS 201 SPS PROPULSION PERFORMANCE PARAMETERS

FUEL FLOW RATE

CK0004 CORR

FIGURE 11

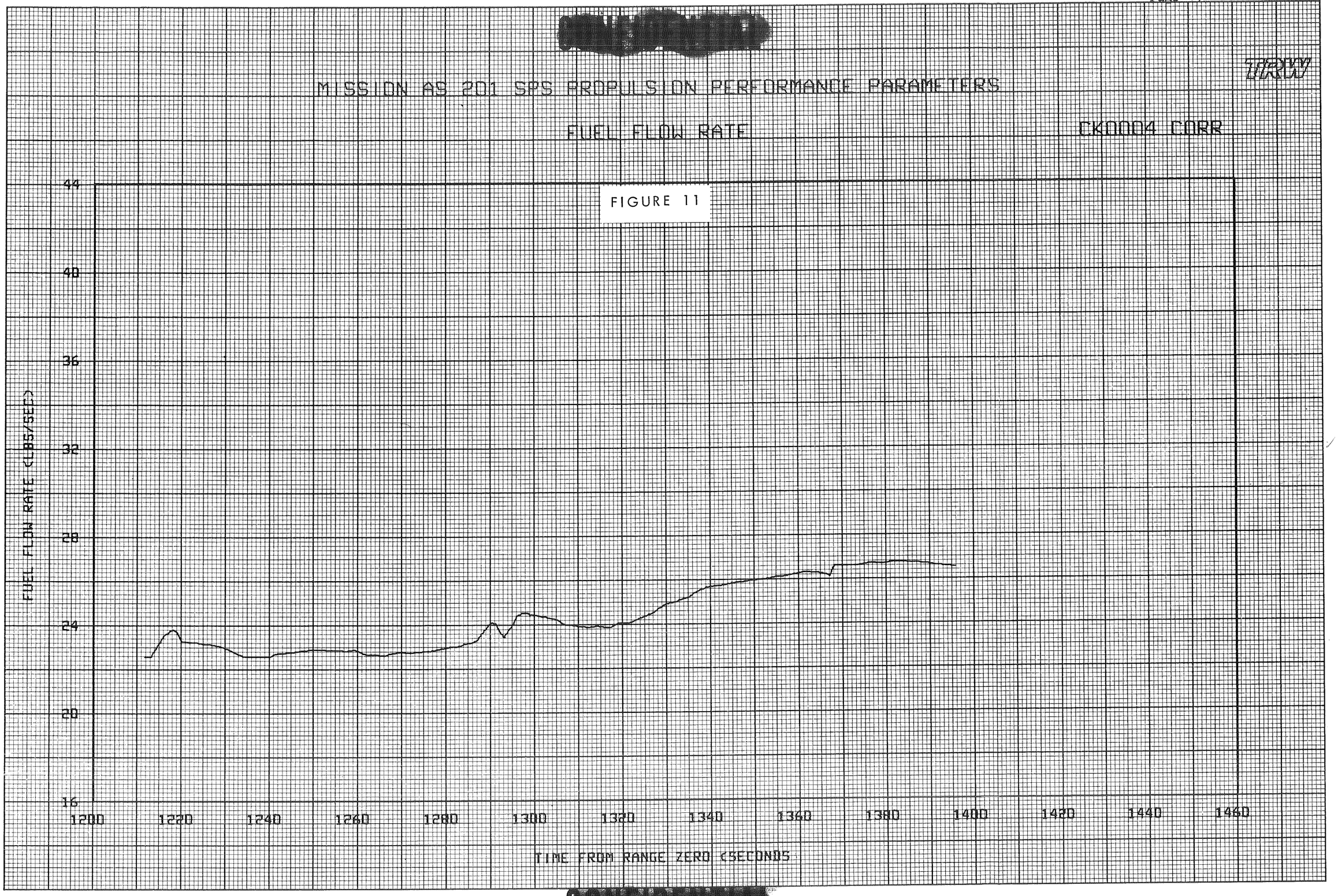


[redacted]

## VII. REFERENCES

1. "Isothermal Pressure Drop for Two-Phase Two Component Flow in a Horizontal Pipe," by R. C. Martinelli, L. M. K. Boelter, T. H. M. Taylor, E. G. Thomsen and E. H. Morrin, Trans., A.S.M.E., vol. 66, 1944

2. "Prediction of Pressure Drop During Forced Circulation Boiling of Water," by R. C. Martinelli and D. B. Nelson, Trans., A.S.M.E., vol. 70, 1948

3. TRW Report 2261-6014-T8-000, "Performance Analysis and Initial SPS Engine Characterization for Test Series L and M," prepared by R. E. Nelson for NASA/MSC, dated 25 February 1966. (Confidential)